SUPPLEMENTAL INFORMATION

Supplemental Figure Legends

Figure S1, related to Figure 1. A) p53 knock-down in *Sirt6* WT and KO primary MEFs. B) Proliferation assay (upper panel) and colony formation assay (lower panel) of shp53-immortalized *Sirt6* WT and KO cells. Error bars indicate SD C) The same cells as in B were injected into the flanks of SCID mice and tumor formation analyzed (representative image).

Figure S2, related to Figure 2. A) Immortalized MEFs derived from Sirt6 conditional mice were infected with adeno-Cre to delete Sirt6 and glucose uptake was measured as indicated in Material and Methods. Error bars indicate SD B) H-RasV12/shp53 transformed MEFs were plated in tripicates in 12-well plates and glucose uptake and C) lactate production was determined using the Glucose Assay Kit and Lactate Assay Kit (BioVision). The results were expressed as a nM/cell. Error bars indicate SEM.

Figure S3, related to Figure 3. A) Western blots showing the activation of ERK and AKT pathways as well as glycolytic gene expression in shp53-immortalized *Sirt6* WT and KO MEFs. B) Representative images of glucose deprivation-induced cell death in *Sirt6* KO and KO-shPDK1 cells.

Figure S4, related to Figure 4. A) Venn diagrams of the top 1000 promoters bound by MYC and its interactors JUN and FOS (left) and scatter plots showing the correlation of all promoters bound by MYC and FOS and MYC and JUN (right). B) The

same as in A but for EZH2 and SIRT6 and MYC. C) Flag-tagged SIRT (2,5 and 6) were co-expressed with MYC in U2OS cells and the presence of MYC was analyzed in the Flag-IPs. D) Real-Time PCR showing the expression of ribosomal genes in immortalized MEFs (n=20) and cells derived from *Sirt6* KO tumors (error bars indicate SEM). E) Glutamine uptake in immortalized (3T3 and shp53) and transformed MEFs (error bars indicate SEM). F) Gls expression in immortalized MEFs and G) colon adenomas from the indicated genotypes (error bars indicate SEM).

Figure S5, related to Figure 5. A) *cMyc* mRNA expression (mean+/- SEM) and B) MYC protein levels in *Sirt6* WT and KO MEFs. C) MYC acetylation levels were analyzed by immunoprecipitating acetylated proteins from *Sirt6* WT and KO ES cells using an acetyl-lysine antibody and and blotting with anti-cMYC antibody. D) ChIP analysis of MYC and E) H3K9ac on the promoters to ribosomal protein genes (error bars indicate SEM).

Figure S6, related to Figure 6. A) SIRT6 copy loss in several types of human cancer collected in The Genome Cancer Atlas (TGCA) portal. B) SIRT6 gene copy number in the cancer cell lines collected in the Cancer Cell Line Encyclopedia (CCLE). C) SIRT6 expression levels in pancreatic and colorectal cancers (Oncomine datasets). D) SIRT6 and glycolytic gene expression levels in colon adenoma (GEO dataset). E) SIRT3 and SIRT6 expression in breast cancer (GEO dataset).

Figure S7, related to Figure 7. A) FDG-PET scanning in mice of the indicated genotypes. B) Representative pictures of colon adenomas in mice of the indicated

genotypes treated or untreated with dichloroacetate (DCA) and western blot showing PDH-E1a phosphorylation in the polyps of the indicated mice.

Extended Experimental Procedures

Cell culture

MEFs were grown in DMEM supplemented with 10% FBS, 2mM L-Glutamine, 0.1mM NEAA, 1mM NaPyr, 20mM HEPES and Pen/Strep. 293T cells were grown in DMEM+10% FBS supplemented with 2mM Glutamine and Pen/Strep.

Western Blot and immunoprecipitation

Western analyis was carried out as previously described (Zhong et al., 2010). The antibodies used are as follows: anti-SIRT6 (Abcam, ab62739), anti-Flag (Sigma), anti-PDK1, anti-LDHa, anti-p53, anti-phospho-AKT (Ser473), anti-total-AKT (Cell Signaling), anti-phospho-ERK (Sigma), anti-ERK (Santa Cruz), anti-phospho-PDH-E1a-Ser293 (Abcam), anti-MYC (Epitomics), anti-actin (Sigma). To analyze SIRT6-MYC interaction, Flag-SIRT6, Flag-SIRT2 and Flag-SIRT5 were co-expressed with MYC in U2OS cells and the Flag-IPs evaluated for the presence of MYC. Endogenous IP were performed in mouse ES cells. Cells were grown to approximately 70% confluency, then washed twice with 1xPBS, and collected in CHAPS buffer (25 mM HEPES, 2mM EGTA, 2.5 mM MgCl2 and 0.3% CHAPS). After 20 minutes of incubation on ice and 20 minutes of centrifugation at 4°C, the supernatants were transferred to fresh tubes. Lysates (1mg) were pre-cleared with 50 ul Protein A Agarose beads (Roche) for two hours and supernatants were collected. IPs were performed by

mixing supernatants with 5 ug of SIRT6 antibody or IgG (Abcam), together with 50 ul of protein A Agarose beads overnight at 4°C. After 3 washes of CHAPS buffer with 150 mM NaCl, the immuno-complexes were eluted by 10 minutes boiling in 4x SDS loading buffer.

Lactate, glutamine and glucose uptake assays

Lactate and glutamine concentration were measured in the media by using the Lactate Assay Kit and the EnzyChrom Glutamine Assay Kit (BioVision), respectively. *In vitro* glucose uptake was carried out as previously described (Zhong et al., 2010).

Luciferase reporter assays

MYC transcriptional activity was determined by luciferase experiments as previously described (Zhong et al., 2010). Briefly, 293T cells were co-transfected with 1μg of pCMV-3xFlag-SIRT6 (or empty vector), 950ng of pMYC-luc (Signosis, Inc., Sunnyvale, CA) and 50ng of pGL3-Renilla. Twenty-four hours after transfection, cells were harvested and luciferase activity was determined using the Dual-Luciferase Reporter Assay system (Promega). An aliquot of the same lysates was used to confirm protein expression of Flag-SIRT6.

RNA extraction and Real-Time RT-PCR

Total RNA was extracted with the TriPure Isolation Reagent (Roche) as described by the manufacturer. For cDNA synthesis, 1 μg of total RNA was retro-transcribed by using the QuantiTect Reverse Transcription Kit (Quiagen). Real-time PCR was performed using the SYBR green master mix (Roche), following the manufacturer's

instructions, with the exception that the final volume was 12.5 µl of SYBR green reaction mix. Real-time monitoring of PCR amplification was performed using the LightCycler 480 detection system (Roche). Data were expressed as relative mRNA levels normalized to the β-*actin* expression level in each sample. The primer sequences can be obtained upon request.

FDG-PET assays

Glucose uptake in tumors was measured as previously described (Zhong et al., 2010). In brief, 15-days after injection of H-RasV12/shp53 cells into SCID mice, animals were imaged using an Inveon (Siemens) small animal scanner. Subjects were fasted for 12 hours prior to imaging and were intravenously injected with approximately 700 µCi ^{18}FDG 45 minutes prior to PET acquisition (Boiselle et al., 1998). CT preceded PET, acquiring 360 cone beam projections, and PET datasets acquired 600 million counts. During CT acquisition, iodine contrast was infused intravenously at a rate of 20 µl/min to enhance intravascular contrast. Data analysis consisted of region of interest analysis on Standard uptake value (SUV) PET images superimposed on anatomic contrast enhanced CT images. Images were analyzed using OsiriX software and FDG-PET data were calculated as SUV_{max} for selected regions of interest. 120-days old APCmin mice were imaged in the same way to analyze *in vivo* adenoma glucose uptake.

Proliferation assay

Cells were plated in triplicates in 12-well plates and cultured in complete media. At the indicated time points, cells were trypsinized and counted. For colony formation assays, 250 cells were plated in 6-well plates and kept in culture for 10-15 days.

Apoptosis assay

Cells were plated in triplicates in 12-well plates and cultured in complete media overnight. Next day, medium was changed to DMEM+10% FBS + 0.3mM Glutamine with or without glucose. After 6 days, cells were collected and stained with Annexin-V (BD) to analyze cell death.

Anchorage independent cell growth

7.500 cells were resuspended in 0.4% agar and plated in triplicates in 6cm-plates containing a 0.8% base agar layer. Colonies were stained with 0.005% Crystal Violet in 2% Methanol and counted.

Viral infection

The following plasmids were use to generate viral particles: pBabe-H-RasV12, pLMS-shp53.1224, pLKO.1-shPDK1 (The MGH RNAi Consortium Library), pLKO.1-shMYC (Open biosciences), pMSCV-3xFlag-SIRT6 (generated by subcloning Flag-SIRT6 from pCMV-3xFlag-SIRT6 to pMSCV-puro). Viral infection was carried out as previously described (Zhong et al., 2010).

Chromatin immunoprecipitation (ChIP) assays

ChIP assays were performed as previously described (Sebastián et al., 2008) with some modifications. Cells were cross-linked with 1% paraformaldehyde for 20 min

at room temperature. The reaction was quenched for 10 min at room temperature by adding 0.125 M glycine. After three washes with 1X PBS, cells were lysed with lysis buffer (1% SDS, 10 mM EDTA pH 8, 50 mM Tris-HCl pH 8) supplemented with protease and deacetylase (TSA) inhibitors. Lysates were sonicated on ice using a Bioruptor sonicator (2 pulses of 10 min, 0.5 min sonication). Size of fragments obtained (between 200 and 1200 bp) was confirmed by electrophoresis. Soluble chromatin was collected after centrifugation at 14,000 rpm at 4°C for 10 min and 1 mg (for MYC IP) or 0.2 mg (for H3K9ac and H3K56ac) of protein was diluted to 1/10 in dilution buffer (1% Triton X-100, 2 mM EDTA, 150 mM NaCl, 20 mM Tris-HCl pH 8.1) supplemented with protease and deacetylase inhibitors. Soluble chromatin (1–5%) was kept as input control.

Soluble chromatin was precleared with 100 µg/ml of salmon sperm (Amersham Biosciences), 2.5 µg/ml of unspecific IgGs, and protein-A-Sepharose at 50% overnight at 4°C in rotation. After centrifugation, supernatants were collected and specific Abs (7.5 µl of MYC –Epitomics-; 3 µl of H3K9ac -Millipore- and H3K56ac -Epitomics) were added. A control was performed with unspecific IgGs (AbCam). Mixtures were incubated at 4°C for 6 h in rotation and then incubated overnight at 4°C in rotation with protein-A-Sepharose at 50% (Roche). Beads were collected and washed sequentially at 4°C for 10 min with TSE I (150 mM NaCl, 0.1% SDS, 1% Triton X-100, 2 mM EDTA, and 20 mM Tris-HCl (pH 8.1)), TSE II (500 mM NaCl, 0.1% SDS, 1% Triton X-100, 2 mM EDTA, and 20 mM Tris-HCl (pH 8.1)), and buffer III (0.25 LiCl, 1% Nonidet P-40, 1% deoxycholate, 1 mM EDTA, and 10 mM Tris-HCl (pH 8.1)). Beads were washed once with 1X PBS by pipetting and

immunoprecipitates were eluted two times (20-min incubation) with elution buffer (0.1 M $NaHCO_3$ and 1% SDS). Reversion of cross-linking was performed overnight by heating samples and input controls at 65°C, and DNA was purified using the QIAquick spin kit (Qiagen). Real time PCR was performed as described above.

Generation of SIRT6 conditional KO mice

The SIRT6 conditional targeting vector was constructed by inserting a Neo cassette (flanked by two Frt sequences) together with SIRT6 exon2 flanked by two loxP sites. Chimeric mice were generated by injecting the targeted ES cells (V6.5) into C57BL6/J blastocysts. The Neo cassette was deleted *in vivo* by crossing the chimeras with a mouse expressing the Flpe endonuclease and the resulting mice were backcrossed for 3 generations with C57BL6/J mice to obtain heterozygous mice that were 97% C57BL6/J background. These mice were interbred to obtain homozygous $SIRT6^{fl/fl}$ mice that were crossed with C57BL/6J-Apc^{Min}/J mice (Jackson Laboratories) and C57BL6/J mice expressing the Cre recombinase under the control of the *Villin 1* promoter (gift from K. Haigis). Cre recombinase exposure leads to exon 2 excision and the appearance of a premature stop codon. Mice were euthanized at 120 days and the intestines harvested and analyzed for the presence of polyps.

Genome-wide overlap of SIRT6 and MYC binding

ChIP-sequencing datasets (aligned to hg19) for *SIRT6* and *MYC* were obtained from Ram *et al.* and Raha *et al*., respectively. We called peaks using Scripture (Guttman et al., 2010) with significance threshold –alpha 0.01 and with –windows parameter

100, 200, 500, 1500, 3000 for *MYC* and 1500, 3000 for *SIRT6.* We removed from our analysis peaks with intensities greater than 3 standard deviations above the mean intensity level, as these likely represent artifacts. We used the intersectBed tool form the BedTools package (Quinlan and Hall, 2010) to determine which genes were bound by *SIRT6* within 3kb and *MYC* within 1kb of the transcription start site as annotated by the UCSC genome browser hg19 RefSeq table (Fujita et al., 2011). In a similar approach to the one used by Rahl et al (Rahl et al., 2010) we ordered each set of binding sites in decreasing order of binding intensity at the promoter regions of the 10% most highly expressed genes. The Venn diagram shows the overlap of the top 1000 bound genes in *MYC* and *SIRT6* datasets. Diagrams were created using the R 'Vennerable' package (http://r-forge.r-project.org/projects/vennerable). Expression data was obtained from Levin et al. (Levin et al., 2009). The RNA-seq reads were aligned to hg19 using TopHat (Trapnell et al., 2009) and FPKM (Fragments per Kilobase of transcript Per Million mapped reads) were calculated using Cufflinks (Trapnell et al., 2010). For functional enrichment analysis of gene sets we used MsigDB (Subramanian et al., 2005) and Panther (Thomas et al., 2003).

In vivo DCA treatment

$SIRT6^{fl/fl}$;V-c;$APC^{min/+}$ and Control;$APC^{min/+}$ mice were treated just after weaning with DCA (5g/l of drinking water) or regular water and euthanized at 108 days of age. Intestines were harvested, fixed were 10% formalin and processed for H&E staining following standard procedures. One polyp of each mouse was collected for protein extraction to analyze PDH-E1a phosphorylation.

Immunohistochemistry

IHC for SIRT6 was performed on tissue microarrays (TMAs). Slides were dewaxed and rehydrated through a series of xylene and alcohol washes. Antigen retrieval was performed by heating under pressure in TE buffer (1mM EDTA, 5mM Tris, pH 8.0) for five minutes in a microwave. Endogenous peroxide was blocked by incubation in 3% hydrogen peroxide (H2O2) for ten minutes. Additional blocking was performed by incubating slides in 1.5% normal horse serum (Vector Laboratories, CA, USA) for one hour. TMAs were incubated with Sirt6 antibody (Lifespan Biosciences, 0.002mg/ml) for 2 hours at 25oC. A negative and positive control was included. Signal was visualised using Envision (DAKO) and 3,3'-diaminobenzidine (DAB, Vector Laboratories).

Histoscore Method

Two observers independently scored tumour cores, as selected by a pathologist, using a weighted histoscore method. The intensity nuclear staining was categorised as negative (0), weak (1), moderate (2) and strong (3) and the percentage of tumour cells within each category estimated. The histoscore was calculated using the following formula:

Histoscore = 0 x % negative tumour cells + 1 x % weakly stained tumour cells + 2 x

% moderately stained tumour cells + 3 x % tumour cells stained strongly.

The histoscore ranged from a minimum of zero to a maximum of 300. Agreement between the two observers was monitored. Cases with discordant results between observers were re-evaluated.

References

Fujita, P.A., Rhead, B., Zweig, A.S., Hinrichs, A.S., Karolchik, D., Cline, M.S., Goldman, M., Barber, G.P., Clawson, H., Coelho, A.*, et al.* (2011). The UCSC Genome Browser database: update 2011. Nucleic Acids Res *39*, D876-882.

Guttman, M., Garber, M., Levin, J.Z., Donaghey, J., Robinson, J., Adiconis, X., Fan, L., Koziol, M.J., Gnirke, A., Nusbaum, C.*, et al.* (2010). Ab initio reconstruction of cell type-specific transcriptomes in mouse reveals the conserved multi-exonic structure of lincRNAs. Nat Biotechnol *28*, 503-510.

Levin, J.Z., Berger, M.F., Adiconis, X., Rogov, P., Melnikov, A., Fennell, T., Nusbaum, C., Garraway, L.A., and Gnirke, A. (2009). Targeted next-generation sequencing of a cancer transcriptome enhances detection of sequence variants and novel fusion transcripts. Genome Biol *10*, R115.

Quinlan, A.R., and Hall, I.M. (2010). BEDTools: a flexible suite of utilities for comparing genomic features. Bioinformatics *26*, 841-842.

Rahl, P.B., Lin, C.Y., Seila, A.C., Flynn, R.A., McCuine, S., Burge, C.B., Sharp, P.A., and Young, R.A. (2010). c-Myc regulates transcriptional pause release. Cell *141*, 432-445.

Subramanian, A., Tamayo, P., Mootha, V.K., Mukherjee, S., Ebert, B.L., Gillette, M.A., Paulovich, A., Pomeroy, S.L., Golub, T.R., Lander, E.S.*, et al.* (2005). Gene set

enrichment analysis: a knowledge-based approach for interpreting genome-wide expression profiles. Proc Natl Acad Sci U S A *102*, 15545-15550.

Sebastian, C., Serra, M., Yeramian, A., Serrat, N., Lloberas, J., and Celada, A. (2008). Deacetylase activity is required for STAT5-dependent GM-CSF functional activity in macrophages and differentiation to dendritic cells. J Immunol *180*, 5898-5906.

Thomas, P.D., Campbell, M.J., Kejariwal, A., Mi, H., Karlak, B., Daverman, R., Diemer, K., Muruganujan, A., and Narechania, A. (2003). PANTHER: a library of protein families and subfamilies indexed by function. Genome Res *13*, 2129-2141.

Trapnell, C., Pachter, L., and Salzberg, S.L. (2009). TopHat: discovering splice junctions with RNA-Seq. Bioinformatics *25*, 1105-1111.

Trapnell, C., Williams, B.A., Pertea, G., Mortazavi, A., Kwan, G., van Baren, M.J., Salzberg, S.L., Wold, B.J., and Pachter, L. (2010). Transcript assembly and quantification by RNA-Seq reveals unannotated transcripts and isoform switching during cell differentiation. Nat Biotechnol *28*, 511-515.

Supplemental Figure S1

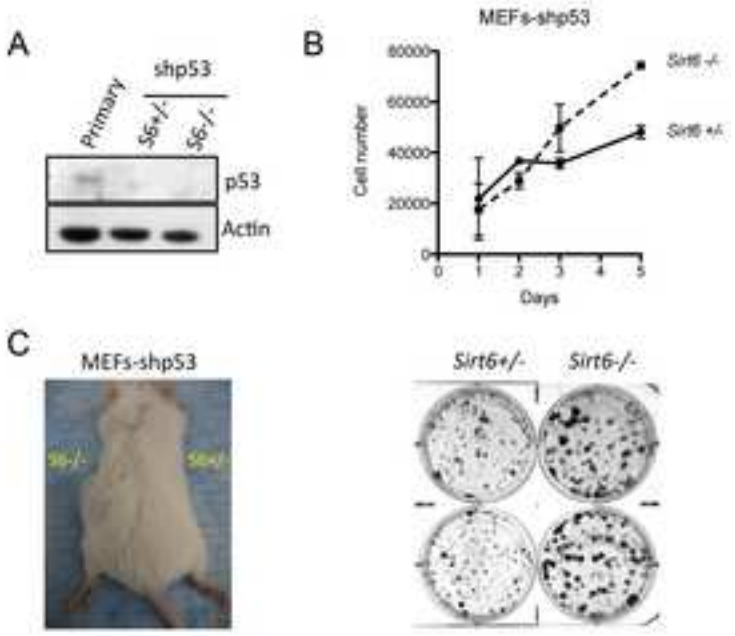

Figure S1

Supplemental Figure S2

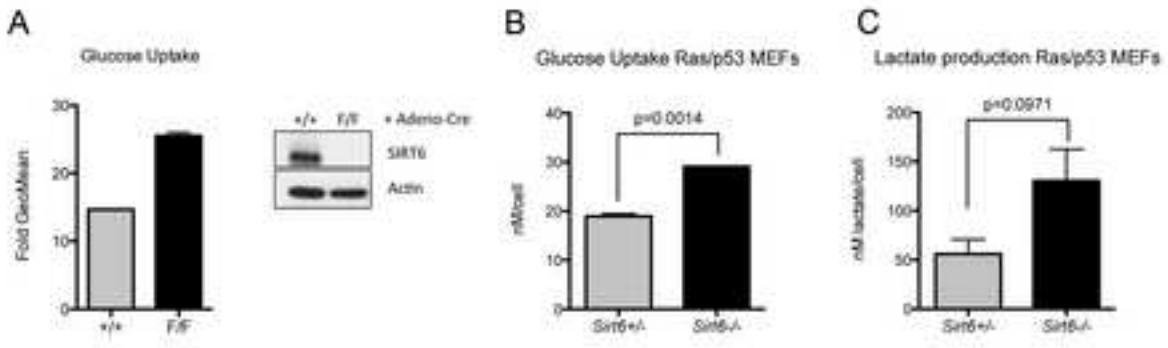

Figure S2

Supplemental Figure S3

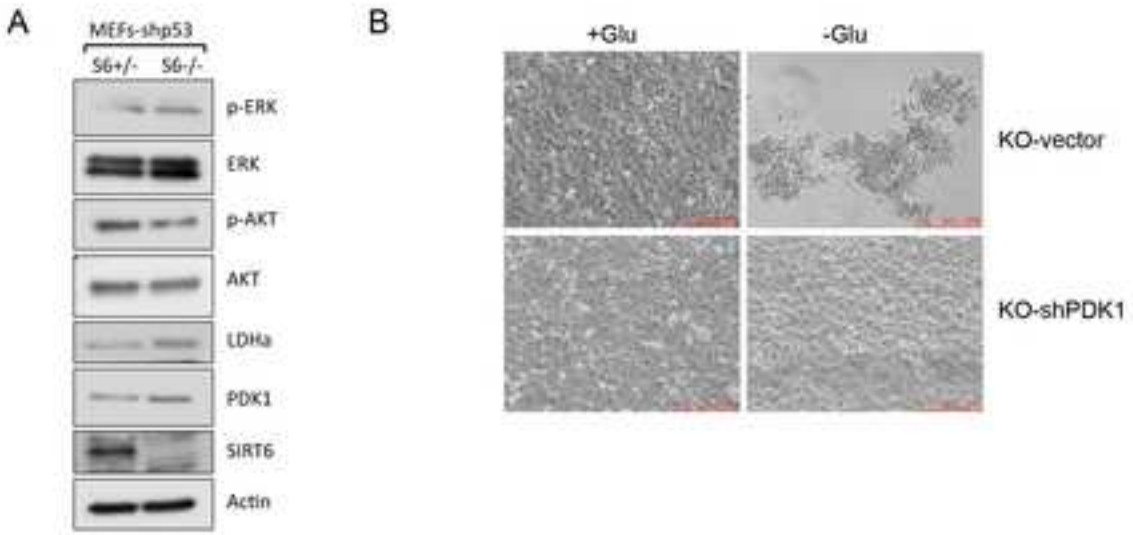

Figure S3

Supplemental Figure S4

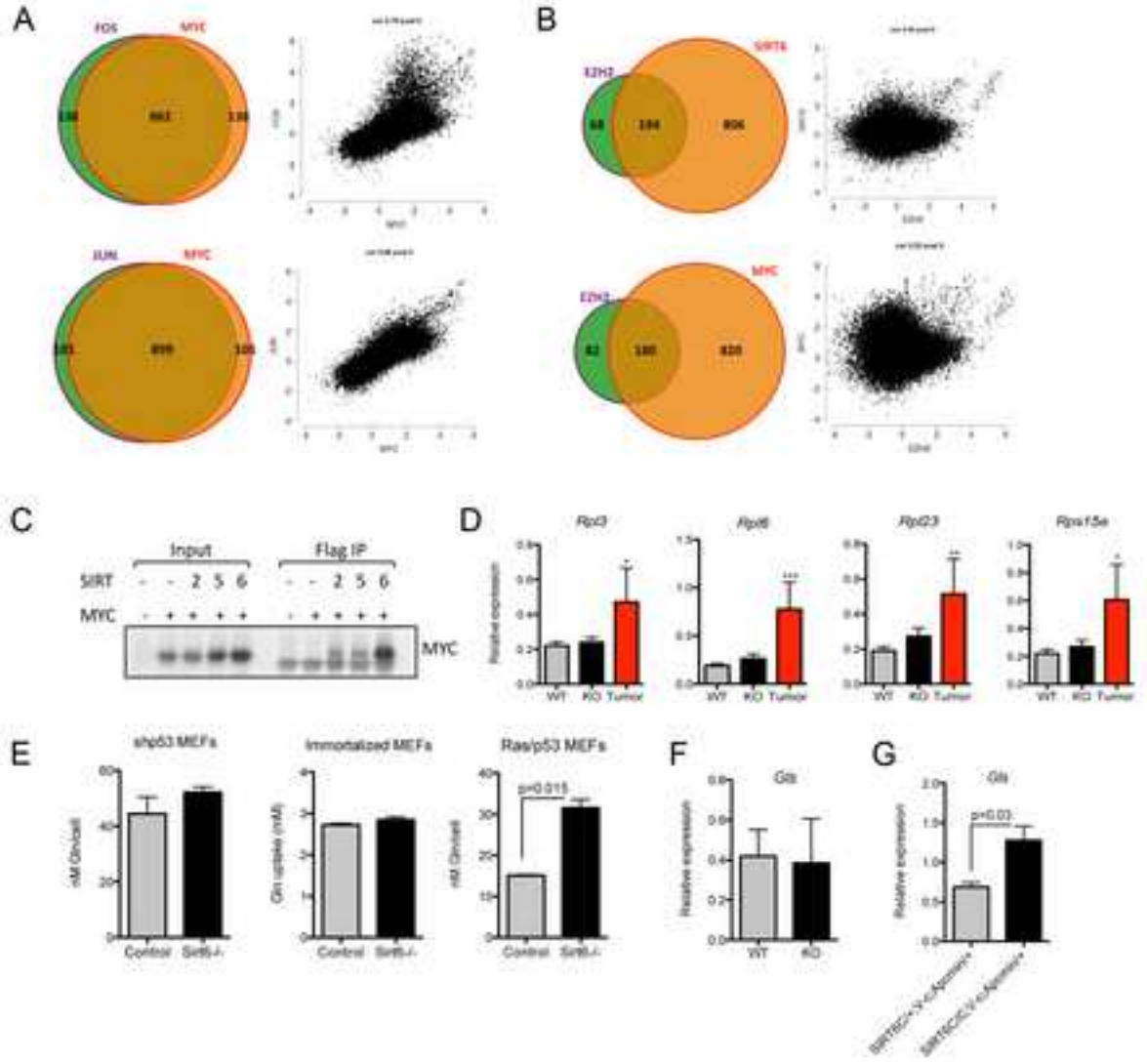

Figure S4

Supplemental Figure S5

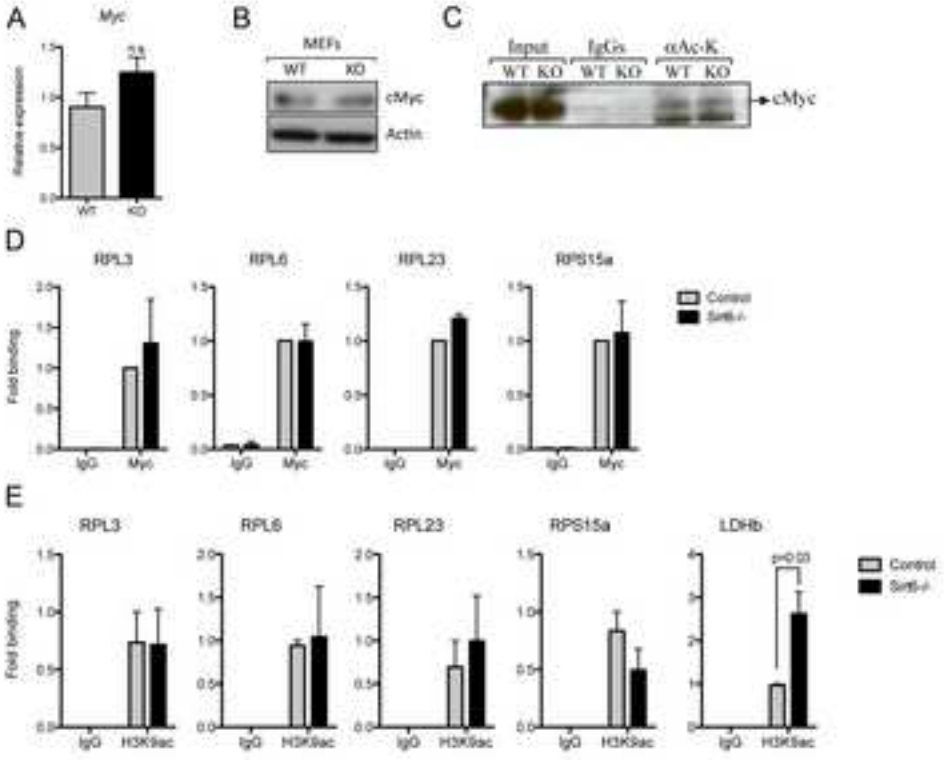

Figure S5

Supplemental Figure S6

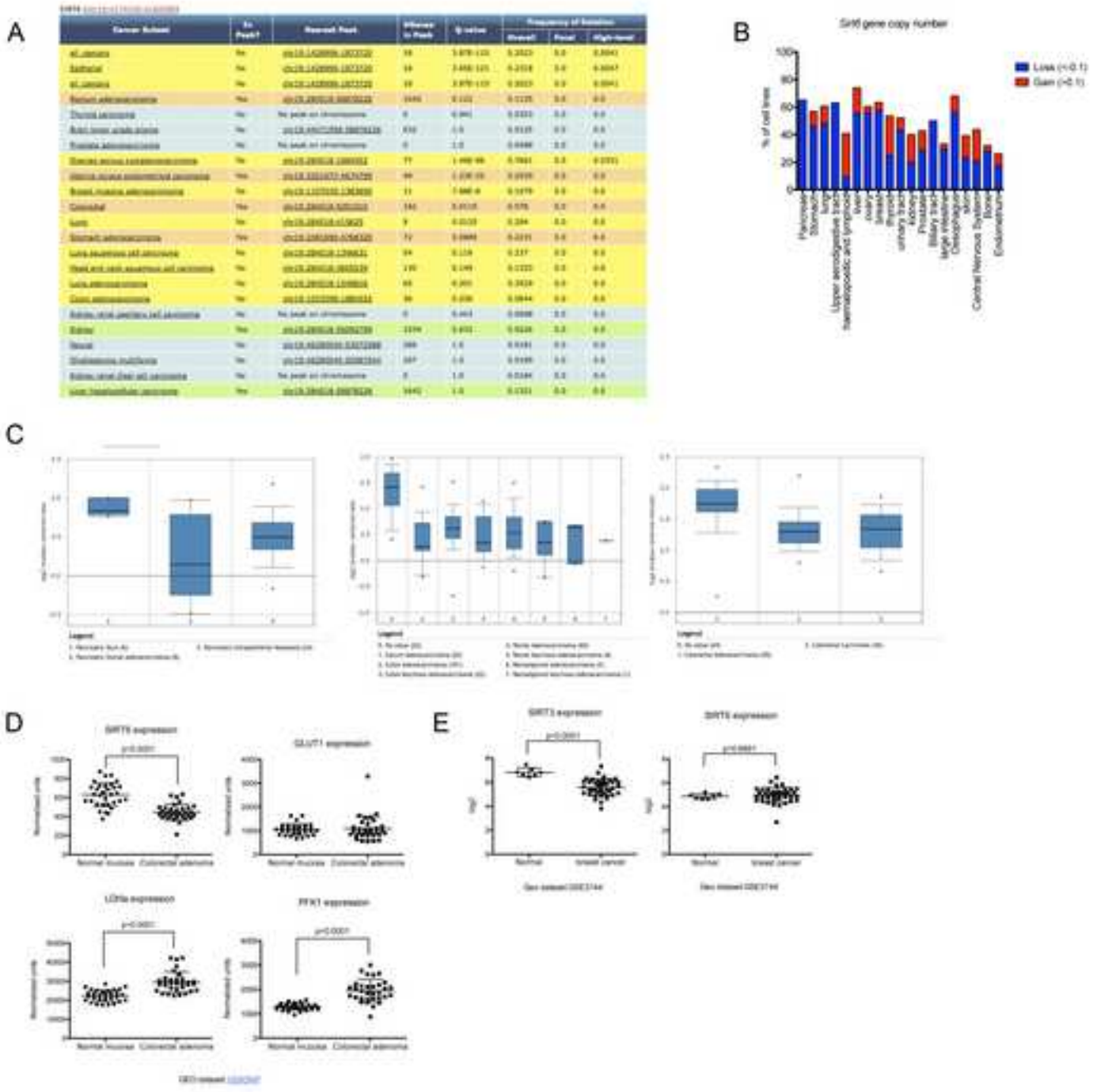

Figure S6

Supplemental Figure S7

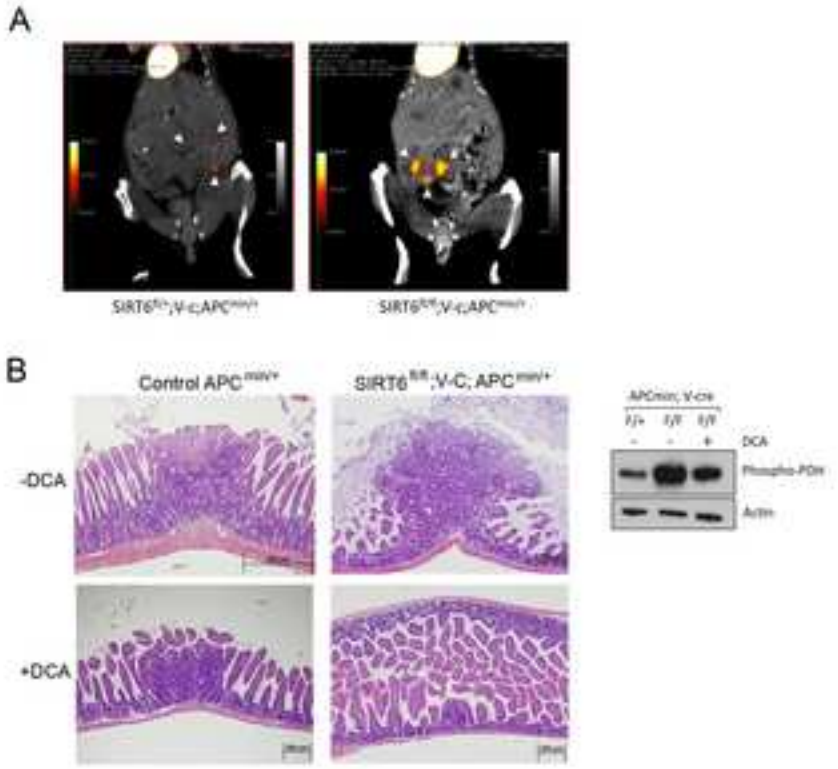

Figure S7